


Orbital Rashba Effect as a Platform for Robust Orbital Photocurrents

T. Adamantopoulos^{1,2,*} M. Merte^{1,2,3} D. Go^{1,3,1} F. Freimuth^{1,3} S. Blügel¹ and Y. Mokrousov^{1,3}

¹*Peter Grünberg Institut, Forschungszentrum Jülich and JARA, 52425 Jülich, Germany*

²*Department of Physics, RWTH Aachen University, 52056 Aachen, Germany*

³*Institute of Physics, Johannes Gutenberg University Mainz, 55099 Mainz, Germany*

 (Received 14 March 2023; revised 3 July 2023; accepted 9 January 2024; published 15 February 2024)

Orbital current has emerged over the past years as one of the key novel concepts in magnetotransport. Here, we demonstrate that laser pulses can be used to generate large and robust nonrelativistic orbital currents in systems where the inversion symmetry is broken by the orbital Rashba effect. By referring to model and first principles tools, we demonstrate that orbital Rashba effect, accompanied by crystal field splitting, can mediate robust orbital photocurrents without a need for spin-orbit interaction even in metallic systems. We show that such nonrelativistic orbital photocurrents are translated into derivative photocurrents of spin when relativistic effects are taken into account. We thus promote orbital photocurrents as a promising platform for optical generation of currents of angular momentum, and discuss their possible applications.

DOI: [10.1103/PhysRevLett.132.076901](https://doi.org/10.1103/PhysRevLett.132.076901)

Introduction.—Recently, we have been witnessing an ever-growing interest in the origins, properties, and prospects of currents of orbital angular momentum (OAM), which often appear to accompany the currents of spin [1–5]. Although suppressed in equilibrium, the orbital degree of freedom can be exploited through the flow of OAM in nonequilibrium—a property that paves the way for moving from conventional spintronics to the upcoming field of orbitronics [6]. Some of the prospects of orbital currents are associated with their often colossal magnitude, and the fact that they emerge even in light materials—abundant, but utterly useless within the paradigms of spintronics that rely on strong spin-orbit interaction (SOI). In the field of orbitronics, the orbital Rashba effect (ORE) has recently emerged as a fruitful playground for understanding and studying orbital properties out of equilibrium [7–11]. Particularly, it has been demonstrated that the formation of chiral orbital textures, arising as a result of broken inversion symmetry at the surfaces and interfaces, results in an orbital version of Rashba-Edelstein effect and generation of colossal orbital currents, which can be efficiently used to generate orbital torques on magnetization [12,13].

Nevertheless, we know very little about the properties of orbital currents in the optical domain. Generally, the physics of optical generation and properties of laser-induced currents appearing at surfaces and interfaces is

now becoming attractive, owing in part to the phenomenon of THz radiation generation with so-called spintronics THz emitters [14,15]. In the context of spinorbitronics inspired optical effects, properties of spin photocurrents also start gaining interest [16–24]. Yet, besides studies of inverse Faraday effect in the orbital channel [25–27] and works on optically ignited orbital dynamics [28–30], orbital photocurrents are largely unexplored, both from the side of fundamental properties as well as their microscopic origins. This is surprising given that a stark redistribution of angular momentum, whose orbital component is bound to be significant, is believed to largely mediate, e.g., demagnetization processes in laser experiments [31,32]. Given the prominent role that orbital currents came to occupy in dc domain, it is thus pertinent to explore the prospects of orbital photocurrents driven by laser and optical pulses. Since the concept of the ORE has been extremely successful in promoting the field of orbitronics, a question arises: can the ORE be taken as a unique starting point for exploring the basic physics of optically induced orbital currents?

Here, we show that the ORE, generally used to describe the crystal symmetry breaking in wide classes of non-centrosymmetric materials, captures the key features of orbital photocurrents. We use tight-binding and *ab initio* methods to show that the magnitude of the OAM photocurrents at surfaces can be colossal, clarifying the role of crystal field splitting (CFS) and orbital Rashba strength for their emergence. We uncover the nonrelativistic nature of orbital photocurrents, and highlight their robustness, which results in stable orbital currents even in systems with vanishing SOI strength. We argue that remarkable properties of orbital photocurrents make them an attractive platform for

Published by the American Physical Society under the terms of the Creative Commons Attribution 4.0 International license. Further distribution of this work must maintain attribution to the author(s) and the published article's title, journal citation, and DOI.

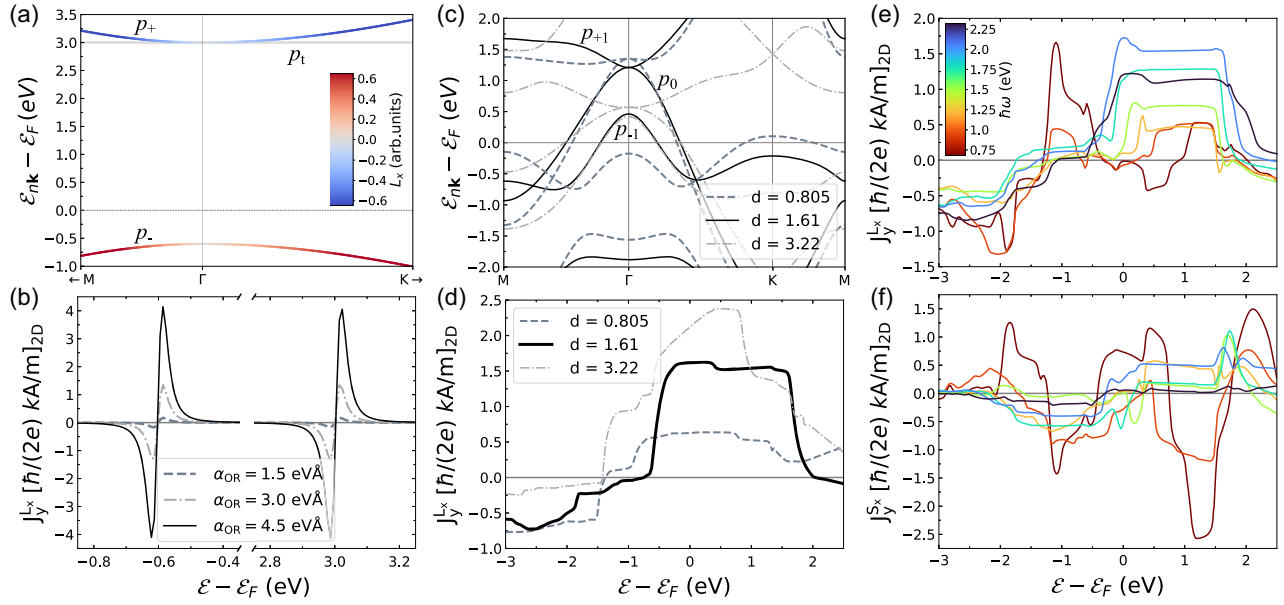


FIG. 1. Orbital photocurrents by ORE. (a) The orbital polarized band structure of the p -orbitals model. The color of the states marks the value of orbital polarization L_x (color bar). (b) The laser-induced orbital photocurrents within the p -orbitals model at $\hbar\omega = 3.6$ eV, in relation to the band filling, for different values of the Rashba constant α_{OR} . (c) Band structure of BiAg_2 surface, without SOI, for different values of separation between Ag and Bi layers (equilibrium value at $d = 1.61$ a.u.). (d) Corresponding dependence of the nonrelativistic orbital photocurrent J_y^x on band filling for $\hbar\omega = 2.25$ eV. (e)–(f) For the BiAg_2 surface with SOI the orbital (e) and spin (f) photocurrents shown as a function of band filling, for different frequencies $\hbar\omega$ (color of the line according to the color scale). In (b), (d)–(f) the $J_y^{L_x/S_x}$ currents arise for light linearly polarized along x , propagating along y , with orbital or spin polarization along x .

further advances in the realm of orbital optospintronics—thus laying a unique road to opto-orbitronics.

Method.—Throughout this Letter, qualitative and quantitative predictions are made by use of Keldysh formalism [18,33] to calculate the second order orbital and spin photocurrents that emerge as a response to a continuous laser pulse of frequency ω . We compute the electronic structure of the realistic orbital Rashba surface from *ab initio* by using the full-potential linearized augmented plane wave FLEUR code [34–36], and employ the Wannier interpolation technique to assess from first principles the laser-induced orbital and spin photocurrents by using Keldysh formalism [23,37,38]. Further computational details and details of the method are given in the Supplemental Material (SM) [39].

Model arguments.—We start by considering a tight-binding model of p orbitals on a two-dimensional triangular lattice (in the xy plane) exposed to a surface potential gradient that mimics the effect of broken inversion symmetry. This model was previously introduced to explain the spin Rashba effect (SRE) at (111) surfaces of noble metals [41], and it was used recently to study orbital magnetism arising from the ORE [8,42,43]. We are interested in the behavior near the Γ point for the case when SOI is absent. In this case, the effective Hamiltonian contains diagonal terms that express the energy separation of the p_x and p_y bands from the p_z band due to the CFS,

while the off-diagonal terms account for the ORE in the general form (an analytic derivation of the tight-binding model is presented in the SM [39,40]):

$$H_{\text{OR}}(\mathbf{k}) = \frac{\alpha_{\text{OR}}}{\hbar} \mathbf{L}^{(p)} \cdot (\hat{\mathbf{z}} \times \mathbf{k}), \quad (1)$$

where α_{OR} is the orbital Rashba constant, and $\mathbf{L}^{(p)}$ is the vector of matrices of OAM operator in the p -orbitals basis set. The $|\phi_{p_{\pm}\mathbf{k}}\rangle$ states that arise carry chiral OAM, evaluated analytically by

$$\langle \phi_{p_{\pm}\mathbf{k}} | \mathbf{L}^{(p)} | \phi_{p_{\pm}\mathbf{k}} \rangle = \pm \hbar \frac{2\alpha_{\text{OR}}}{\Delta_{\text{CF}}} \hat{\mathbf{z}} \times \mathbf{k}, \quad (2)$$

where Δ_{CF} is the value of CFS. The chiral distribution of OAM in k space is the trademark of ORE. A typical band structure of the model is shown in Fig. 1(a) in the vicinity of the Γ point [39]. The distance between the p_{\pm} states is tuned by the values of α_{OR} and Δ_{CF} , whereas α_{OR} also influences the curvature of the p_{\pm} bands. As expected from Eq. (2), the p_{\pm} states have OAM of opposite sign, while a tangential p_t state carries no OAM.

It is known that the ORE unleashes the linear in the field current-induced orbital magnetization [11]. In the next step, we utilize the Keldysh formalism to demonstrate the generation of laser-induced orbital photocurrents within

the ORE. In Fig. 1(b) we show the orbital photocurrent J_y^{Lx} component as a function of band filling. The light frequency is set at $\hbar\omega = 3.6$ eV and matches exactly the energy difference between the p_{\pm} states at Γ . The calculated orbital response is remarkably sharp and strong with the peaks located slightly above and below the energies of the p_{\pm} states. Since the ORE drives orbital photocurrents already without SOI, the effect should strongly depend on the orbital Rashba strength. Indeed, as shown in Fig. 1(b), the orbital photoresponse increases drastically with the value of α_{OR} . For the value of $\alpha_{OR} = 3.0$ eV Å, which corresponds to the case of BiAg₂(111) surface alloy [44], the predicted magnitude of the orbital photocurrent reaches a very large value of about 1600 ($\hbar/2e$)(A/m).

Realistic systems.—To explore the possibility of generating large orbital photocurrents in realistic systems, we choose a prominent representative of the class of strong Rashba surfaces: the BiAg₂ alloy [44,45]. It was demonstrated experimentally that Bi/Ag Rashba interfaces host spin-to-charge conversion processes that lead to THz emission [46,47]. Previously calculated charge photocurrents on this system were in agreement with the experimental findings [38]. The symmetry behavior of the calculated orbital photocurrents agrees with the symmetry predictions of the effective nonmagnetic spin Rashba model [18]. For simplicity, in the following we restrict our discussion only to J_y^{Lx} and J_y^{Sx} components of the orbital and spin photocurrents, respectively, which arise for light linearly polarized along the x axis. Additional components are presented in the SM [39].

We start discussing by studying the case without SOI. The sp -orbital hybridization at the BiAg₂ surface is known to give rise to the prominent ORE [10], which is reflected in its characteristic band structure, shown with black lines in Fig. 1(c) for the equilibrium lattice constant: the main features are identical to that of the orbital Rashba model, with p_{+1} and p_0 bands of Bi degenerate at Γ point and split off from the p_{-1} band. Remarkably, we observe that, in accordance to the predictions of the model analysis from above, the ORE gives rise to very large *nonrelativistic* orbital currents in response to laser light, as shown for the case of $\hbar\omega = 2.25$ eV as a function of band filling in Fig. 1(d). Here, for the equilibrium structural configuration, we not only observe a magnitude of the order of 1500 ($\hbar/2e$)(A/m) for J_y^{Lx} , but also witness a remarkable robustness of the orbital current to the changes in band filling, reminiscent of a band insulator, where such behavior is expected when the Fermi energy is varied within the band gap [48–51].

In particular, the width of the observed plateau in energy can be roughly associated with the difference in energy between p_{-1} , p_0 , and p_{+1} bands: the plateau starts from the region of flat p_{-1} and p_0 states around $[-1; -0.5]$ eV and goes up to the energy region of flat p_{+1} states around $+1.6$ eV. Outside of this region, the orbital response is generally suppressed. We correlate the $p_{\pm 1}$ separation with

the orbital current plateau by changing the distance between the Ag and Bi layers, resulting in modifications in the effective orbital Rashba strength and CFS, subsequently having a strong effect on the energy dependence of J_y^{Lx} . Indeed, as seen in Fig. 1(d), the plateau size follows the effective separation between the orbitally polarized bands: by doubling the distance, the p_{+1} band goes down in energy with respect to $p_{-1,0}$ states, but not as significantly as for the case of decreased interlayer distance. In both cases, while modifications in α_{OR} change the magnitude of the response, as predicted by the model, the modifications in the CFS together with α_{OR} reduce the effective plateau size.

While clearly we can achieve gigantic nonrelativistic orbital currents, it is important to explore the influence of the universally present in real solids SOI. Therefore, the following, particularly relevant for our heavy test system, questions arise: (i) what is the impact of SOI on magnitude and robustness of the orbital photocurrents? (ii) Would the orbital currents become irrelevant when SOI-driven spin photocurrents come into play? The latter have been recently shown to become very prominent in two-dimensional materials with broken inversion symmetry [19–23,38].

To answer the first question, we consider SOI and compute the orbital photocurrents for various frequencies, presenting the results as a function of band filling in Fig. 1(e). Comparing the J_y^{Lx} curves obtained for $\hbar\omega = 2.25$ eV with and without SOI, remarkably reveals little difference. This signifies orbital currents as slightly sensitive to changes in the band structure by SOI, than to further decisive effect of CFS and ORE, which determine the main features of the bands on a larger than SOI energy scale. Upon decreasing the frequency, less transitions across differently polarized p states are activated, and thus the width of the plateau becomes smaller while the finer features of the p states unveil. For example, a larger peak in J_y^{Lx} just above -1 eV at $\hbar\omega = 0.75$ eV is explained by transitions among p_0 and p_{-1} states around that energy that are deactivated at higher frequencies.

A more drastic effect of SOI lies in promoting the spin physics within the Rashba realm: if without SOI each state of the system is spin-degenerate, SOI splits this degeneracy, making the overall electronic structure spin-polarized in k space—a picture often referred to as the SRE [52]. Consequently, the combined effect of ORE and SOI unleashes the light-induced spin photocurrents [18]. To compare the orbital and spin photocurrents in BiAg₂, we compute the latter, presenting the results in Fig. 1(f). We conclude that although overall their magnitude is nominally similar, in the robust region of band filling between 0 and $+2$ eV the orbital currents are dominating by far, except for smaller frequencies of light. For example, for $\hbar\omega = 2.0$ eV the achieved orbital photoconductivity value of $\sigma_{xx}^{yLx} \approx 3000$ ($\hbar/2e$) $\mu\text{A}/\text{V}^2$ is compared to a corresponding spin photoconductivity value of $\sigma_{xx}^{ySx} \approx 500$ ($\hbar/2e$) $\mu\text{A}/\text{V}^2$.

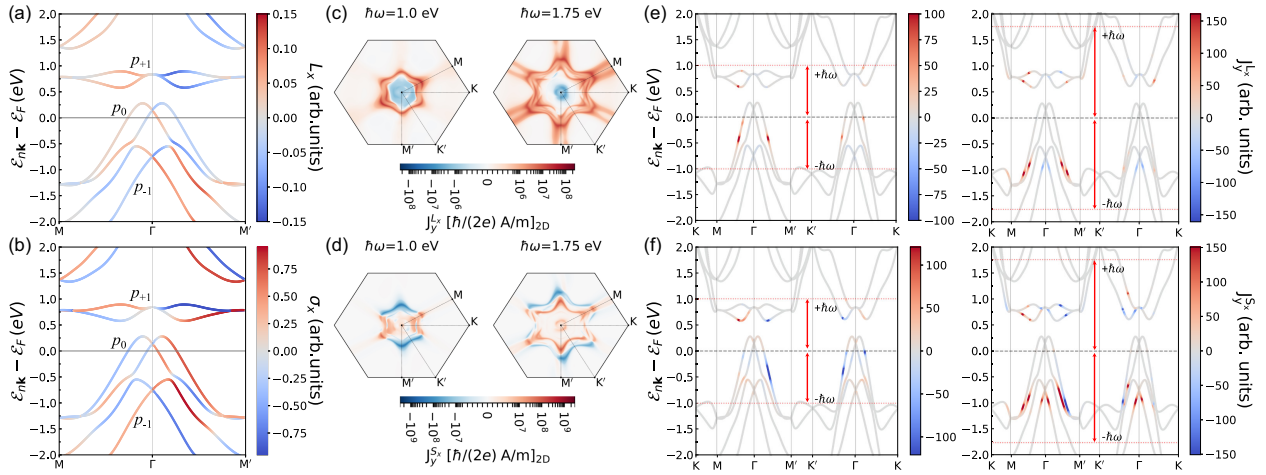


FIG. 2. Microscopies of orbital photocurrents. (a),(b) Orbitally polarized (a) and spin-polarized (b) band structure of the BiAg₂ surface with SOI, with the states of distinct orbital symmetry marked as $p_{\pm 1}$, p_0 . (c),(d) Reciprocal space distribution of integrated (c) orbital and (d) spin photocurrents, at the shifted Fermi energy level $\mathcal{E}'_F = \mathcal{E}_F + 0.9$ eV. (e),(f) Band-resolved two-band contributions of (e) orbital and (f) spin photocurrents. The responses are calculated for light frequencies of $\hbar\omega = 1.00$ eV [left panels in (c)–(f)] and $\hbar\omega = 1.75$ eV [right panels in (c)–(f)]. The presented component arises for light linearly polarized along the x axis and flows along the y axis with orbital or spin polarization along the x -axis. In (e),(f) the horizontal dotted red lines at ± 1.0 eV (left panels) and at ± 1.75 eV (right panels) denote the laser pulse energy.

We remark that at higher frequencies corresponding to the CFS energy scale the spin photocurrents become suppressed, whereas at lower frequencies of the SRE energy scale they become comparable to the orbital photocurrents, hereby introducing a physical mechanism to apply frequency control of spin or orbital nature of optically excited angular momentum currents. Upon reducing the SOI strength by hand, the magnitude of the spin currents is respectively reduced (not shown), vanishing in the limit of zero SOI. Given that among Rashba materials BiAg₂ is among the heaviest, at lighter Rashba surfaces, such as that of oxygenated Cu [11], the orbital character will dominate the nature of the photoinduced currents of angular momentum in a wide frequency range.

To understand deeper the properties of orbital photocurrents we scrutinize their anatomy in reciprocal space. We start by looking at the distribution of orbital and spin photocurrents in k space, J_y^{Lx} and J_y^{Sx} in Figs. 2(c) and 2(d), respectively, assuming the shifted Fermi energy of 0.9 eV above the true Fermi level—which falls right into the middle of the plateau region and roughly corresponds to the position of p_{+1} band—for the frequencies of 1.0 and 1.75 eV. Initially, the distributions are similar in structure: upon increasing the frequency, the regions of strong contributions move further away from the Γ point, a signature of active electronic transitions moving closer to the Brillouin zone boundaries and high-symmetry lines. Clearly, the distribution of the photocurrents of angular momentum probes the shape of the valence band that launches the transitions into the p_{+1} band. However, one remarkable feature sticks out: while at larger frequencies the sign of the orbital photocurrents is predominantly

uniform throughout the Brillouin zone, the photocurrents of spin exhibit a characteristic behavior where the regions of positive and negative contributions reflect each other in shape. This explains why, contrary to orbital photocurrents, the spin photocurrents are strongly suppressed when integrated over the k space.

Analyzing in detail the electronic structure clarifies the root of key difference between two types of currents. Figures 2(a) and 2(b) show the bands of BiAg₂ with SOI along $\text{M}\Gamma\text{M}'$, colored by the magnitude of the orbital (a) and spin (b) polarization of the states along x . In comparison to nonrelativistic bands of Fig. 1(c), we see a very prominent splitting of the states caused by the strong SOI. Remarkably, while the SOI splitting keeps the orbital polarization sign of the SOI-split states the same along a given k path, instead, the spin polarization of the states alternates sign. This effect, evident for p_{+1} and p_{-1} bands around $+0.75$ eV and -1 eV respectively, stems from the fact that basic features of the orbital polarization are already set by the combined effect of ORE and CFS onto which SOI acts as a perturbation. The spin case is drastically different: an alternating spin polarization is direct consequence of the k -dependent SOI-mediated coupling of electron's spin to the surface gradient, being the essence of SRE. Hence, the orbital photocurrents originating in ORE enhance their magnitude, while SRE suppresses the spin photocurrents—with suppression becoming stronger as the splitting between the alternating-in-sign regions in k space becomes smaller with decreasing SOI.

The band-resolved decomposition of the photocurrents also clearly shows fingerprints of this behavior. In Figs. 2(e) and 2(f) we plot the contributions of so-called resonant

two-state transitions [53,54] to orbital (e) and spin (f) photocurrents along the high-symmetry lines: irrespective of light frequency chosen (1.0 eV or 1.75 eV), an alternating-in-sign behavior is much more characteristic of a spin photocurrent than of its orbital counterpart, in accord to the qualitative behavior of state polarization. The latter plots also provide a key to understand the aforementioned quantizationlike features in orbital photocurrents. It is important to realize that the narrow p_{+1} group of states stands energetically well-separated from the rest of orbitally polarized valence and conduction bands, a primary consequence of the CFS at the ORE surface. Then light with a given frequency launches electronic transitions among the p_{+1} band and occupied states that are lower by about $\hbar\omega$ in energy; see Figs. 2(e) and 2(f). Respectively, changes in frequency probe the structure of the valence p_0 and p_{-1} states—an effect we speculated to take place above. However, since the energetics of electronic transitions is already set by the magnitude of CFS and light frequency, varying the band filling within a certain interval plays only a minor role, which gives rise to a robust plateau in the orbital response. Note that quasiquantization plateaus in orbital photocurrent are irrespective to the presence of a global band gap in the spectrum apparent in Fig. 2, since the robust behavior emerges already in non-relativistic limit where the system is manifestly metallic.

Discussion.—Given the observed properties of orbital photocurrents, it is tempting to imagine their possible impact in optical magnetism. Firstly, their role for demagnetization properties has to be explored. In fact, first experiments suggest that an interaction of magnetization with laser pulses may trigger orbital currents [55,56], which can even exhibit a long-range nature [57]. We thus speculate that orbital photocurrents may interact with magnetic properties in an unexpected way. For example, would it be feasible to exploit orbital photocurrents for exerting sizeable optical torques on the magnetization that take place on the femtosecond timescale? This may prove indispensable in, e.g., all-optical antiferromagnetic switching schemes that do not rely on intrinsically slower demagnetization processes. The nonrelativistic nature of orbital photocurrents would, on the other hand, open a whole new palette of opportunities associated with material realization of optical phenomena, traditionally escaping the search as generators of sizeable spin-based processes. At the same time, the origin of orbital photocurrents in the crystal structure and key features of chemical composition would enable a reliable and robust control of opto-orbital properties, promoting new possibilities in our struggle to master light-matter interaction.

This work was supported by the Deutsche Forschungsgemeinschaft (DFG, German Research Foundation)—TRR 173/2—268565370 (project A11), TRR 288—422213477 (project B06), and the Sino-German research project DISTOMAT (MO 1731/10-1). This project has received

funding from the European Union’s Horizon 2020 research and innovation programme under the Marie Skłodowska-Curie Grant Agreement No. 861300. We also gratefully acknowledge the Jülich Supercomputing Centre and RWTH Aachen University for providing computational resources under projects jiff40 and jara0062.

*Corresponding author: t.adamantopoulos@fz-juelich.de

- [1] B. A. Bernevig, T. L. Hughes, and S.-C. Zhang, Orbitronics: The intrinsic orbital current in p -doped silicon, *Phys. Rev. Lett.* **95**, 066601 (2005).
- [2] T. Tanaka, H. Kontani, M. Naito, T. Naito, D. S. Hirashima, K. Yamada, and J. Inoue, Intrinsic spin Hall effect and orbital Hall effect in $4d$ and $5d$ transition metals, *Phys. Rev. B* **77**, 165117 (2008).
- [3] H. Kontani, T. Tanaka, D. S. Hirashima, K. Yamada, and J. Inoue, Giant orbital Hall effect in transition metals: Origin of large spin and anomalous Hall effects, *Phys. Rev. Lett.* **102**, 016601 (2009).
- [4] D. Go, D. Jo, C. Kim, and H.-W. Lee, Intrinsic spin and orbital Hall effects from orbital texture, *Phys. Rev. Lett.* **121**, 086602 (2018).
- [5] D. Jo, D. Go, and H.-W. Lee, Gigantic intrinsic orbital Hall effects in weakly spin-orbit coupled metals, *Phys. Rev. B* **98**, 214405 (2018).
- [6] D. Go, D. Jo, H.-W. Lee, M. Kläui, and Y. Mokrousov, Orbitronics: Orbital currents in solids, *Europhys. Lett.* **135**, 37001 (2021).
- [7] S. R. Park, C. H. Kim, J. Yu, J. H. Han, and C. Kim, Orbital-angular-momentum based origin of Rashba-type surface band splitting, *Phys. Rev. Lett.* **107**, 156803 (2011).
- [8] J.-H. Park, C. H. Kim, J.-W. Rhim, and J. H. Han, Orbital Rashba effect and its detection by circular dichroism angle-resolved photoemission spectroscopy, *Phys. Rev. B* **85**, 195401 (2012).
- [9] J.-H. Park, C. H. Kim, H.-W. Lee, and J. H. Han, Orbital chirality and Rashba interaction in magnetic bands, *Phys. Rev. B* **87**, 041301(R) (2013).
- [10] D. Go, J.-P. Hanke, P. M. Buhl, F. Freimuth, G. Bihlmayer, H.-W. Lee, Y. Mokrousov, and S. Blügel, Toward surface orbitronics: Giant orbital magnetism from the orbital Rashba effect at the surface of sp-metals, *Sci. Rep.* **7**, 46742 (2017).
- [11] D. Go, D. Jo, T. Gao, K. Ando, S. Blügel, H.-W. Lee, and Y. Mokrousov, Orbital Rashba effect in a surface-oxidized Cu film, *Phys. Rev. B* **103**, L121113 (2021).
- [12] D. Go, F. Freimuth, J.-P. Hanke, F. Xue, O. Gomonay, K.-J. Lee, S. Blügel, P. M. Haney, H.-W. Lee, and Y. Mokrousov, Theory of current-induced angular momentum transfer dynamics in spin-orbit coupled systems, *Phys. Rev. Res.* **2**, 033401 (2020).
- [13] D. Go and H.-W. Lee, Orbital torque: Torque generation by orbital current injection, *Phys. Rev. Res.* **2**, 013177 (2020).
- [14] T. Seifert, S. Jaiswal, U. Martens, J. Hannegan, L. Braun, P. Maldonado, F. Freimuth, A. Kronenberg, J. Henrizi, I. Radu, E. Beaurepaire, Y. Mokrousov, P. M. Oppeneer, M. Jourdan, G. Jakob, D. Turchinovich, L. M. Hayden, M. Wolf, M. Münzenberg, M. Kläui, and T. Kampfrath,

- Efficient metallic spintronic emitters of ultrabroadband terahertz radiation, *Nat. Photonics* **10**, 483 (2016).
- [15] E. T. Papaioannou and R. Beigang, THz spintronic emitters: A review on achievements and future challenges, *Nanophotonics* **10**, 1243 (2021).
- [16] E. Y. Sherman, A. Najmaie, and J. E. Sipe, Spin current injection by intersubband transitions in quantum wells, *Appl. Phys. Lett.* **86**, 122103 (2005).
- [17] J. Yin and H. Peng, Asymmetry allows photocurrent in intrinsic graphene, *Nat. Nanotechnol.* **14**, 105 (2019).
- [18] F. Freimuth, S. Blügel, and Y. Mokrousov, Charge and spin photocurrents in the Rashba model, *Phys. Rev. B* **103**, 075428 (2021); F. Freimuth, S. Blügel, and Y. Mokrousov, Laser-induced currents of charge and spin in the Rashba model, [arXiv:1710.10480](https://arxiv.org/abs/1710.10480).
- [19] H. Xu, H. Wang, J. Zhou, and J. Li, Pure spin photocurrent in non-centrosymmetric crystals: Bulk spin photovoltaic effect, *Nat. Commun.* **12**, 4330 (2021).
- [20] R.-C. Xiao, D.-F. Shao, Y.-H. Li, and H. Jiang, Spin photogalvanic effect in two-dimensional collinear antiferromagnets, *npj Quantum Mater.* **6**, 35 (2021).
- [21] R. Fei, W. Song, L. Pusey-Nazzaro, and L. Yang, PT -symmetry-enabled spin circular photogalvanic effect in anti-ferromagnetic insulators, *Phys. Rev. Lett.* **127**, 207402 (2021).
- [22] X. Mu, Y. Pan, and J. Zhou, Pure bulk orbital and spin photocurrent in two-dimensional ferroelectric materials, *npj Comput. Mater.* **7**, 61 (2021).
- [23] M. Merte, F. Freimuth, T. Adamantopoulos, D. Go, T. G. Saunderson, M. Kläui, L. Plucinski, O. Gomonay, S. Blügel, and Y. Mokrousov, Photocurrents of charge and spin in monolayer Fe_3GeTe_2 , *Phys. Rev. B* **104**, L220405 (2021).
- [24] S. Hayami, M. Yatsushiro, and H. Kusunose, Nonlinear spin Hall effect in PT -symmetric collinear magnets, *Phys. Rev. B* **106**, 024405 (2022).
- [25] M. Battiato, G. Barbalinardo, and P. M. Oppeneer, Quantum theory of the inverse Faraday effect, *Phys. Rev. B* **89**, 014413 (2014).
- [26] M. Berritta, R. Mondal, K. Carva, and P. M. Oppeneer, *Ab initio* theory of coherent laser-induced magnetization in metals, *Phys. Rev. Lett.* **117**, 137203 (2016).
- [27] J. Zhou, Photo-magnetization in two-dimensional sliding ferroelectrics, *npj 2D Mater. Appl.* **6**, 15 (2022).
- [28] T. Satoh, R. Iida, T. Higuchi, Y. Fujii, A. Koreeda, H. Ueda, T. Shimura, K. Kuroda, V. I. Butrim, and B. A. Ivanov, Excitation of coupled spin-orbit dynamics in cobalt oxide by femtosecond laser pulses, *Nat. Commun.* **8**, 638 (2017).
- [29] M. Matthiesen, J. R. Hortensius, S. Mañas-Valero, I. Kapon, D. Dumcenco, E. Giannini, M. Šiškins, B. A. Ivanov, H. S. J. van der Zant, E. Coronado, A. B. Kuzmenko, D. Afanasiev, and A. D. Caviglia, Controlling magnetism with light in a zero orbital angular momentum antiferromagnet, *Phys. Rev. Lett.* **130**, 076702 (2023).
- [30] M. J. Grzybowski, C. F. Schippers, O. Gomonay, K. Rubi, M. E. Bal, U. Zeitler, A. Kozioł-Rachwał, M. Szpytma, W. Janus, B. Kurowska, S. Kret, M. Gryglas-Borysiewicz, B. Koopmans, and H. J. M. Swagten, Antiferromagnetic hysteresis above the spin-flop field, *Phys. Rev. B* **107**, L060403 (2023).
- [31] W. Töws, G. Stegmann, and G. M. Pastor, Spin and orbital symmetry breakings central to the laser-induced ultrafast demagnetization of transition metals, *Symmetry* **15**, 457 (2023).
- [32] G. Stegmann, W. Töws, and G. M. Pastor, Ultrafast magnetization and energy flow in the laser-induced dynamics of transition metal compounds, *Phys. Rev. B* **107**, 054410 (2023).
- [33] F. Freimuth, S. Blügel, and Y. Mokrousov, Laser-induced torques in metallic ferromagnets, *Phys. Rev. B* **94**, 144432 (2016).
- [34] D. Wortmann *et al.*, FLEUR, Zenodo (2023), [10.5281/zenodo.7891361](https://zenodo.org/record/7891361).
- [35] J. P. Perdew, K. Burke, and M. Ernzerhof, Generalized gradient approximation made simple, *Phys. Rev. Lett.* **77**, 3865 (1996).
- [36] C. Li, A. J. Freeman, H. J. F. Jansen, and C. L. Fu, Magnetic anisotropy in low-dimensional ferromagnetic systems: Fe monolayers on Ag(001), Au(001), and Pd(001) substrates, *Phys. Rev. B* **42**, 5433 (1990).
- [37] G. Pizzi *et al.*, Wannier90 as a community code: New features and applications, *J. Phys. Condens. Matter* **32**, 165902 (2020).
- [38] T. Adamantopoulos, M. Merte, D. Go, F. Freimuth, S. Blügel, and Y. Mokrousov, Laser-induced charge and spin photocurrents at the BiAg_2 surface: A first-principles benchmark, *Phys. Rev. Res.* **4**, 043046 (2022).
- [39] See Supplemental Material at <http://link.aps.org/supplemental/10.1103/PhysRevLett.132.076901> for an analytic derivation of the presented tight-binding model, further computational details, details of the first principles methods, and additional components of the orbital and spin photocurrents, which includes Refs. [10,18,33–38,40].
- [40] D. Go, Orbital dynamics and transport in spintronics, Ph.D. thesis, Pohang University of Science and Technology, 2019.
- [41] L. Petersen and P. Hedegård, A simple tight-binding model of spin-orbit splitting of sp-derived surface states, *Surf. Sci.* **459**, 49 (2000).
- [42] B. Kim, C. H. Kim, P. Kim, W. Jung, Y. Kim, Y. Koh, M. Arita, K. Shimada, H. Namatame, M. Taniguchi, J. Yu, and C. Kim, Spin and orbital angular momentum structure of Cu(111) and Au(111) surface states, *Phys. Rev. B* **85**, 195402 (2012).
- [43] J. Hong, J.-W. Rhim, C. Kim, S. Ryong Park, and J. Hoon Shim, Quantitative analysis on electric dipole energy in Rashba band splitting, *Sci. Rep.* **5**, 13488 (2015).
- [44] C. R. Ast, J. Henk, A. Ernst, L. Moreschini, M. C. Falub, D. Pacilé, P. Bruno, K. Kern, and M. Gironi, Giant spin splitting through surface alloying, *Phys. Rev. Lett.* **98**, 186807 (2007).
- [45] C. Carbone, P. Moras, P. M. Sheverdyaeva, D. Pacilé, M. Papagno, L. Ferrari, D. Topwal, E. Vescovo, G. Bihlmayer, F. Freimuth, Y. Mokrousov, and S. Blügel, Asymmetric band gaps in a Rashba film system, *Phys. Rev. B* **93**, 125409 (2016).
- [46] M. B. Jungfleisch, Q. Zhang, W. Zhang, J. E. Pearson, R. D. Schaller, H. Wen, and A. Hoffmann, Control of terahertz emission by ultrafast spin-charge current conversion at Rashba interfaces, *Phys. Rev. Lett.* **120**, 207207 (2018).

- [47] C. Zhou, Y. P. Liu, Z. Wang, S. J. Ma, M. W. Jia, R. Q. Wu, L. Zhou, W. Zhang, M. K. Liu, Y. Z. Wu, and J. Qi, Broadband terahertz generation via the interface inverse Rashba-Edelstein effect, *Phys. Rev. Lett.* **121**, 086801 (2018).
- [48] L. M. Canonico, T. P. Cysne, A. Molina-Sanchez, R. B. Muniz, and T. G. Rappoport, Orbital Hall insulating phase in transition metal dichalcogenide monolayers, *Phys. Rev. B* **101**, 161409(R) (2020).
- [49] T. P. Cysne, M. Costa, L. M. Canonico, M. B. Nardelli, R. B. Muniz, and T. G. Rappoport, Disentangling orbital and valley Hall effects in bilayers of transition metal dichalcogenides, *Phys. Rev. Lett.* **126**, 056601 (2021).
- [50] T. P. Cysne, S. Bhowal, G. Vignale, and T. G. Rappoport, Orbital Hall effect in bilayer transition metal dichalcogenides: From the intra-atomic approximation to the Bloch states orbital magnetic moment approach, *Phys. Rev. B* **105**, 195421 (2022).
- [51] M. Zeer, D. Go, J. P. Carbone, T. G. Saunderson, M. Redies, M. Kläui, J. Ghabboun, W. Wulfhekel, S. Blügel, and Y. Mokrousov, Spin and orbital transport in rare-earth dichalcogenides: The case of EuS_2 , *Phys. Rev. Mater.* **6**, 074004 (2022).
- [52] Y. A. Bychkov and E. I. Rashba, Properties of a 2D electron gas with lifted spectral degeneracy, *JETP Lett.* **39**, 66 (1984), http://jetpletters.ru/ps/1264/article_19121.shtml.
- [53] Y. Zhang, H. Ishizuka, J. van den Brink, C. Felser, B. Yan, and N. Nagaosa, Photogalvanic effect in Weyl semimetals from first principles, *Phys. Rev. B* **97**, 241118(R) (2018).
- [54] Y. Zhang, T. Holder, H. Ishizuka, F. de Juan, N. Nagaosa, C. Felser, and B. Yan, Switchable magnetic bulk photovoltaic effect in the two-dimensional magnet CrI_3 , *Nat. Commun.* **10**, 3783 (2019).
- [55] Y. Xu, F. Zhang, Y. Liu, R. Xu, Y. Jiang, H. Cheng, A. Fert, and W. Zhao, Inverse orbital Hall effect discovered from light-induced terahertz emission, [arXiv:2208.01866](https://arxiv.org/abs/2208.01866).
- [56] P. Wang, Z. Feng, Y. Yang, D. Zhang, Q. Liu, Z. Xu, Z. Jia, Y. Wu, G. Yu, X. Xu, and Y. Jiang, Inverse orbital Hall effect and orbitronic terahertz emission observed in the materials with weak spin-orbit coupling, *npj Quantum Mater.* **8**, 28 (2023).
- [57] T. S. Seifert, D. Go, H. Hayashi, R. Rouzegar, F. Freimuth, K. Ando, Y. Mokrousov, and T. Kampfrath, Time-domain observation of ballistic orbital-angular-momentum currents with giant relaxation length in tungsten, *Nat. Nanotechnol.* **18**, 1132 (2023).